

## SPECTROSCOPIC STUDY OF 2-PHENYL-THIAZOLE -4-YL-METHYL-QUINOLINIUM IODINE

A. PÎRNĂU<sup>1</sup>, M. BOGDAN<sup>1</sup>, M. MIC<sup>1\*</sup>, M. PALAGE<sup>2</sup>, R. A. VARGA<sup>3</sup>

<sup>1</sup>Institute for Research and Development of Isotopic and Molecular Technologies, RO-400293,  
Cluj-Napoca, Romania

<sup>2</sup>Iuliu Hațieganu University of Medicine and Pharmacy, Department of Therapeutical Chemistry,  
Ion Creanga 12, RO-400010, Cluj-Napoca, Romania

<sup>3</sup>Babeş-Bolyai University, Faculty of Chemistry and Chemical Engineering, Arany Janos 11,  
RO-400028 Cluj-Napoca, Romania

\*corresponding author: mihaela.mic@itim-cj.ro

*Received February 5, 2014*

This Nowadays, the design of new compounds able to deal with resistant bacteria, having new structures and new targets of action, has become one of the most important areas in the antibacterial research purpose. Thiazolic quaternary ammonium salts were synthesized and assessed for antimicrobial, antispasmodic or spasmodic activity. Quinolinium compounds presented a good activity and for spectroscopic study was selected phenyl-thiazole-4-yl-methyl-quinolinium iodide (2PTMQI). The molecular structure of the compound 2PTMQI has been studied by X-ray diffraction technique and <sup>1</sup>H and <sup>13</sup>C NMR spectroscopy. X-ray diffraction technique indicates that 2PTMQI crystallizes like a cationic - anionic pair, the organic cation being the quinoline fragment and a phenylthiazole moiety linked by a methylene group and the corresponding iodine anion. The 1D and 2D NMR spectra of 2PTMQI were obtained at 300 K in DMSO solution and the chemical shifts of <sup>1</sup>H and <sup>13</sup>C nuclei were measured relative to TMS.

*Key words:* quaternary ammonium compounds; NMR spectroscopy; X-ray diffraction.

### 1. INTRODUCTION

Structural investigations on compounds of biomedical and pharmacological interest are increasingly reported in the last years in the scientific literature. For this goal, spectroscopic methods like NMR and X-ray diffraction were successful used in order to a good understanding of their pharmacological activity [1-3]. The treatment of infectious diseases is an important and challenging problem due to a combination of factors, including emerging infectious diseases and the increasing number of multi-drug resistant microbial pathogens. Bacterial resistance has become a serious public health problem, demanding new classes of antibacterial

agents. The quaternary ammonium group is present in antiseptic, antispasmodic or spasmodic compounds [4-7], in addition the thiazole ring constitute the core structure of some biologically interesting compounds like antimicrobial, anti-diabetic, anti-inflammatory or analgesic drugs [8, 9]. Thus, long chain quaternary ammonium compounds exert antibacterial activity against both Gram-positive and Gram-negative bacteria, as well as against some pathogenic species of fungi and protozoa. These quaternary ammonium compounds, in general, have toxic effects toward mammalian cells. In humans and animals they are considered too toxic for systemic applications, but acceptable for topical applications.

In this context a new class of thiazolic quaternary ammonium salts has been recently synthesized by us and after antibacterial, antiseptic and screening tests, we concluded that 2PTMQI compound has the most intense activity (Figure 1).

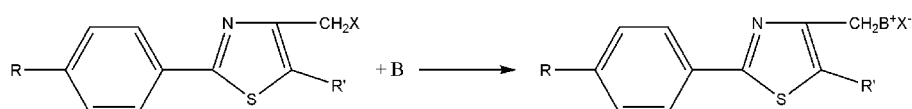


Fig. 1 – The scheme of synthesis of 2-phenyl-thiazole-4-yl-methyl-quinolinium iodide compound (2PTMQI); where **R**: H, CH<sub>3</sub>, Cl; **R'**: H, Br; **B**: 3-methyl-pyridine, quinoline, N-methyl-piperidine, N-methyl-morpholine; **X**: Cl, I.

The synthesis of 2PTMQI compound was performed by the alkylation of some nitrogen heterocycles, with halogen compounds, having in their structure 2-Aryl-thiazolic system [4, 10]. The bactericide activity of the new compound has been evaluated against two strains of germs: *Staphylococcus aureus* and *Escherichia coli* and the effect on the smooth muscles were tested using guinea pig isolated ileum experimental model [11].

The correlation of the obtained results with the chemical structure of the compounds, revealed the importance of the substituent in the 4 position of the thiazole ring for the biological activity. The quinolinium salt 2PTMQI presented a bactericide activity and a significative contractile effect on the guinea pig isolated ileum [10, 11].

## 2. EXPERIMENTAL

X-ray diffraction measurements were performed on a Bruker Smart Apex CCD diffractometer at 297 K. The intensity data were collected using graphite monochromated Mo-K $\alpha$  radiation ( $\lambda = 0.71073 \text{ \AA}$ ). The structures were solved by direct methods using the SHELX-97 software package and refined by full-matrix least-squares procedures on  $F^2$ . All non-hydrogen atoms were refined with anisotropic displacement parameters [12]. All C-bound H atoms were placed in calculated positions (C-H = 0.93–0.97  $\text{\AA}$ ) and treated using a riding model with  $U_{iso} = 1.2U_{eq}(\text{C})$  for aryl H atoms.

The drawings were created using the ORTEP3 and Diamond programs [13, 14]. The crystal data, further details of the experimental conditions and the structure refinement parameters for 2PTMQI are given in Table 1.

Crystallographic data for the structure reported in this paper have been deposited with the Cambridge Crystallographic Data Centre as Supplementary Publication CCDC 795856.

Table 1

Crystal data and structure refinement for 2PTMQI

Empirical formula	C <sub>19</sub> H <sub>15</sub> IN <sub>2</sub> S
Formula weight	430.29
Temperature, K	297(2)
Wavelength, Å	0.71073
Crystal system	Triclinic
Space group	<i>P</i> -1
<i>a</i> / Å	8.044(4)
<i>b</i> / Å	8.479(4)
<i>c</i> / Å	13.559(6)
$\alpha$ / °	82.078(8)
$\beta$ / °	83.526(8)
$\gamma$ / °	74.350(7)
Volume / Å <sup>3</sup>	879.2(7)
<i>Z</i>	2
Calculated density / g cm <sup>-3</sup>	1.625
Absorption coefficient / mm <sup>-1</sup>	1.940
F(000)	424
Crystal size / mm <sup>3</sup>	0.37 x 0.25 x 0.22
$\theta$ range for data collection / °	2.51 - 25.00
Limiting indices	-9 ≤ <i>h</i> ≤ 9 -10 ≤ <i>k</i> ≤ 10 -16 ≤ <i>l</i> ≤ 16
Reflection collected/unique	8538 / 3085 [R <sub>int</sub> = 0.0361]
Completeness to $\theta$	99.6
Refinement method	Full-matrix least-squares on <i>F</i> <sup>2</sup>
Data/restraints/parameters	3085 / 0 / 208
Goodness-of-fit on <i>F</i> <sup>2</sup>	1.112
<i>R</i> <sub>1</sub> , <i>wR</i> <sub>2</sub> [ <i>I</i> > 2 $\sigma$ ( <i>I</i> )]	0.0320, 0.0705
Largest diff. peak and hole / e Å <sup>-3</sup>	0.425 and -0.323

The NMR experiments were performed at 500 MHz for <sup>1</sup>H and 125 MHz for <sup>13</sup>C, on a Bruker Avance III, spectrometer. The NMR spectra were recorded in solution at 300 K and all chemical shifts were measured relative to TMS. The

sample was prepared by dissolving the synthesized powder of the 2PTMQI compound in DMSO- $d_6$  ( $\delta_H = 2.51$  ppm and ( $\delta_C = 40.03$  ppm). The types of measurements performed on this molecule were:  $^1\text{H}$  NMR,  $^{13}\text{C}$  NMR,  $^{13}\text{C}$ -DEPT NMR,  $^1\text{H}$ - $^1\text{H}$  COSY NMR and  $^1\text{H}$ - $^{13}\text{C}$  HSQC NMR.

For  $^1\text{H}$  NMR experiment, 32 scans were collected into 65 K data points over a 4250 Hz spectral window, using an excitation pulse of 10.1  $\mu\text{s}$ . Proton decoupled  $^{13}\text{C}$  NMR spectra were obtained, using an excitation pulse of 8  $\mu\text{s}$  and 2048 scans were collected into 65 K data points over a 29760 Hz spectral window. The  $^{13}\text{C}$ -DEPT NMR spectrum was obtained use the 4096 scans were collected into 65 K data points over a 16400 Hz. The 2D  $^1\text{H}$ - $^1\text{H}$  COSY NMR spectra were acquired using 8 scans and a Bruker standard program (pulse program cosygf45). Each spectrum consisted of a matrix of 2048/512 data points covering a spectral width of 2250 Hz. The 2D  $^1\text{H}$ - $^{13}\text{C}$  HSQC NMR spectra were acquired using the pulse program hsqcetgp. Each spectrum consisted of a matrix of 2048 ( $^1\text{H}$ ) / 1024 ( $^{13}\text{C}$ ) data points covering a spectral width of 2250 Hz ( $^1\text{H}$ ) / 16400 Hz ( $^{13}\text{C}$ ) and collecting 8 scans.

### 3. RESULTS AND DISCUSSIONS

#### *Solid-state structures*

X-ray diffraction technique is widely applied to provide information on the structure-based drug design approaches during drug discovery stages thus helping in the design of physically and biopharmaceutically relevant crystalline materials [15, 16].

The crystal and molecular structure of 2PTMQI (see Figure 2 for ORTEP diagrams and atom numbering schemes), was determined by single-crystal X-ray diffraction technique. Suitable 2PTMQI crystals for X-ray diffraction analysis were grown by solvent diffusion.

In solid state, the organic cation, consisting of a quinoline fragment and a phenylthiazole moiety linked by a methylene group, crystallizes with an iodine anion. The cations are linked in a dimeric unit through strong C—H $\cdots\pi$  intermolecular interactions between one methylene hydrogen from one fragment and the phenyl group of another [H(31) $\cdots$ Cg1 = 2.619(1) Å]. The two cations are disposed in a head-to-tail arrangement with the phenylthiazole moieties and the quinoline parts in trans species being perfectly parallel to each other. There is a 76.90(5) $^\circ$  between the two constituents of the cation. Weaker C—H $\cdots\pi$  intermolecular interactions, between one phenyl hydrogen and all carbon ring of the quinolin fragment [H(34) $\cdots$ Cg2 = 2.971(1) Å], bind the dimers in a ribbon like arrangement along the b axis. The iodine anion form weak hydrogen bond like interaction with the other methylene hydrogen of each organic cation [H(30) $\cdots$ I(38) = 3.110(1) Å].

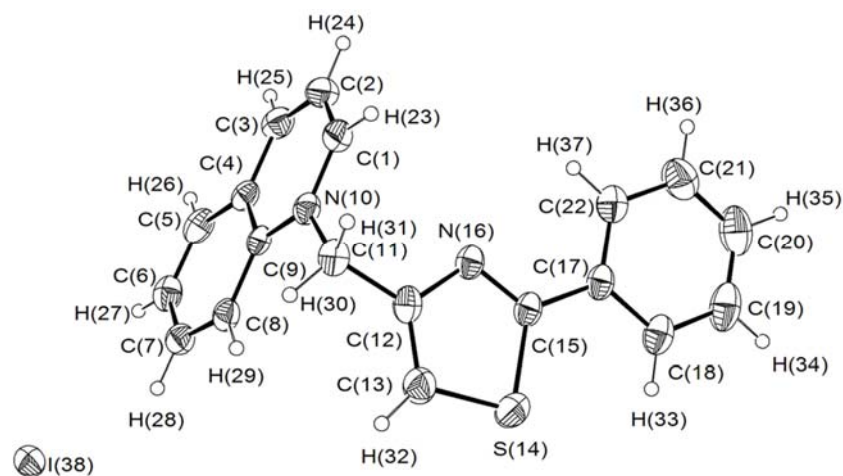


Fig. 2 – ORTEP diagram and atom numbering scheme of 2PTMQI with displacement ellipsoids at 50% probability level.

The quinoline fragments from different ribbons are also parallel, in a head-to-tail arrangement and with a half of aromatic ring offset forming a perfect stack. In Figure 3 is presented the crystal packing of 2PTMQI along the crystallographic *a* axis (a) and along the crystallographic *b* axis (b).

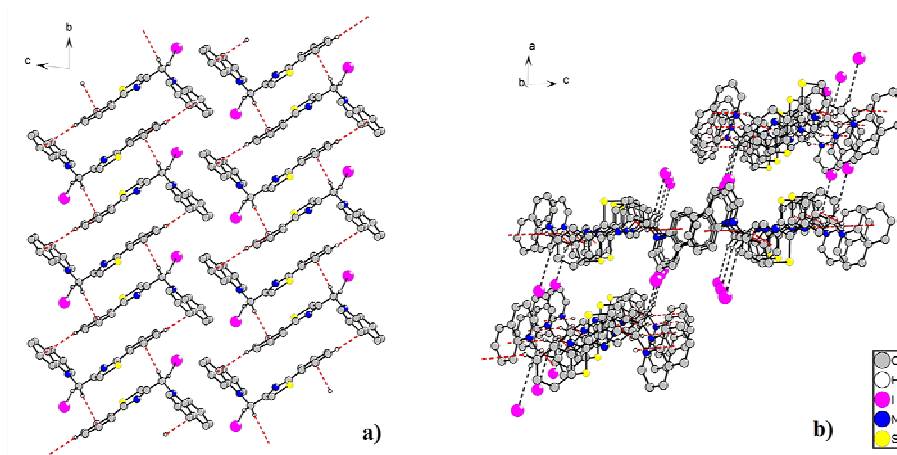


Fig. 3 – Crystal packing of 2PTMQI along the crystallographic *a* axis (a) and along the crystallographic *b* axis (b).

### *NMR spectroscopy*

The NMR measurements of 2PTMQI were performed on liquid state samples, using DMSO-*d*<sub>6</sub> as deuterated solvent (gives a residual peak of water at

about 3.37 ppm in  $^1\text{H}$  NMR spectrum) [17]. To determine how accurately is the molecular structure of 2PTMQI, we performed NMR measurements of the type:  $^1\text{H}$  NMR,  $^{13}\text{C}$  NMR,  $^{13}\text{C}$ -DEPT NMR,  $^1\text{H}$ - $^1\text{H}$  COSY NMR and  $^1\text{H}$ - $^{13}\text{C}$  HSQC NMR. For all NMR spectra, we used atom numbering scheme presented in Figure 2.

In the  $^1\text{H}$  NMR spectrum (see Figure 4), the aromatic ring protons (H33, H34, H35, H36, H37) gives signals in 7–8 ppm range. The multiplet between 7.787–7.806 ppm is assigned to the H33 and H37 protons. Also, the multiplet between 7.456–7.469 ppm is assigned to H34, H35 and H36 protons. The singlet peak at 8.161 ppm is assigned to H32 and the singlet peak at 6.553 ppm is assigned to methylene group (H30 and H31). The protons of the quinoline group give signals between 8 – 10 ppm: H23 and H29 appear as doublet of doublets, H25 and H26 as doublets, H24 as quartet, H27 and H28 as triplets. The values of peak integrals nicely reproduce the number of protons in each group.

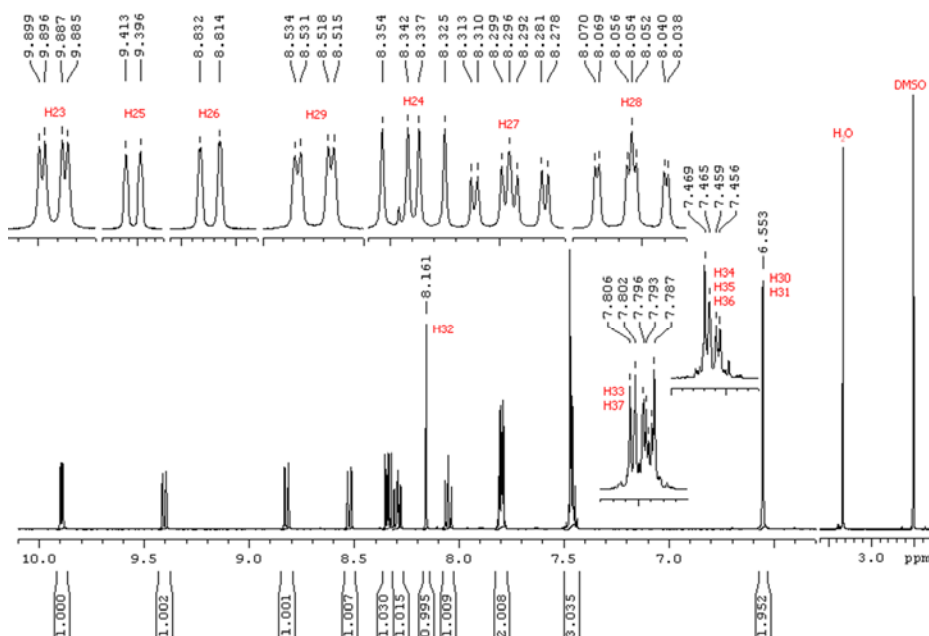


Fig. 4 –  $^1\text{H}$  NMR spectrum of 2PTMQI molecule; inset: details zoom.

For a good assignment of  $^1\text{H}$  NMR spectrum, we take into account the two-dimensional  $^1\text{H}$ - $^1\text{H}$  COSY NMR spectrum (CORrelation SpectroscopY) which describes the interactions between neighbor protons (Figure 5a and 5b) [18]. We used this experiment to put in evidence the existing proton homonuclear spin – spin coupling in 2PTMQI molecule.

In Figure 5a are highlighted the interactions between protons of the methylene group (H30 and H31) with H32 and H23 and also the interactions between aromatic ring protons H33, H37 with H33, H35 and H36. Interactions

between other neighboring protons in the 2PTMQI molecule are highlighted in Figure 5b. Thus, we have revealed the following interactions: H23 with H24 and H25; H25 with H24 and H26; H26 with H27 and H28; H29 with H27 and H28; H27 with H28. Also, it can be seen that H32 does not interact with another proton.

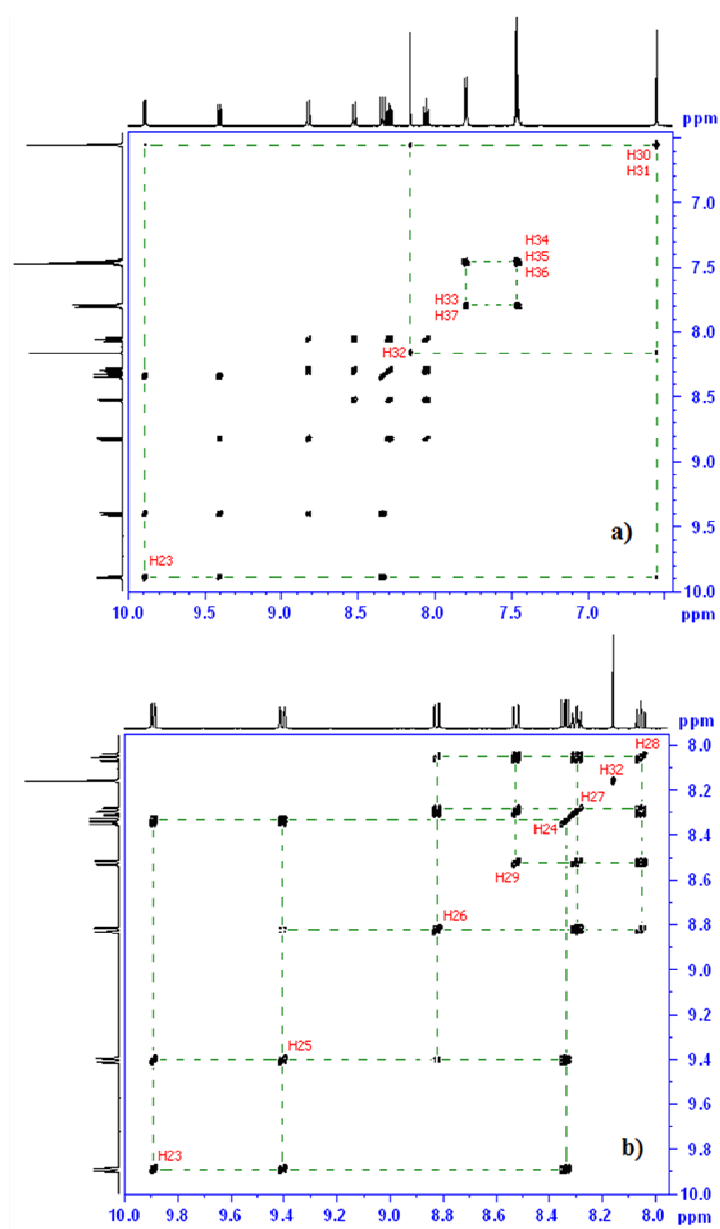


Fig. 5 –  $^1\text{H}$ - $^1\text{H}$  COSY NMR spectrum of 2PTMQI molecule (a); details zoom of 8 – 10 ppm (b).

The assignment of  $^{13}\text{C}$  NMR chemical shifts of 2PTMQI molecule is presented in Figure 6. This spectrum shows all signals, inclusive for quaternary carbon atoms. Also, we can observe the signal of  $^{13}\text{C}$  from DMSO- $d_6$  solvent and signal of  $^{13}\text{C}$  of the methylene group (C11). To highlight the quaternary carbon atoms and carbon atom of the methylene group, we performed a  $^{13}\text{C}$ -DEPT NMR measurement (Figure 7). In this type of experiment the quaternary carbon atoms (C4, C9, C12, C15 and C17) cannot be seen and the carbon atom of the methylene group (C11) appears upside down in the spectrum.

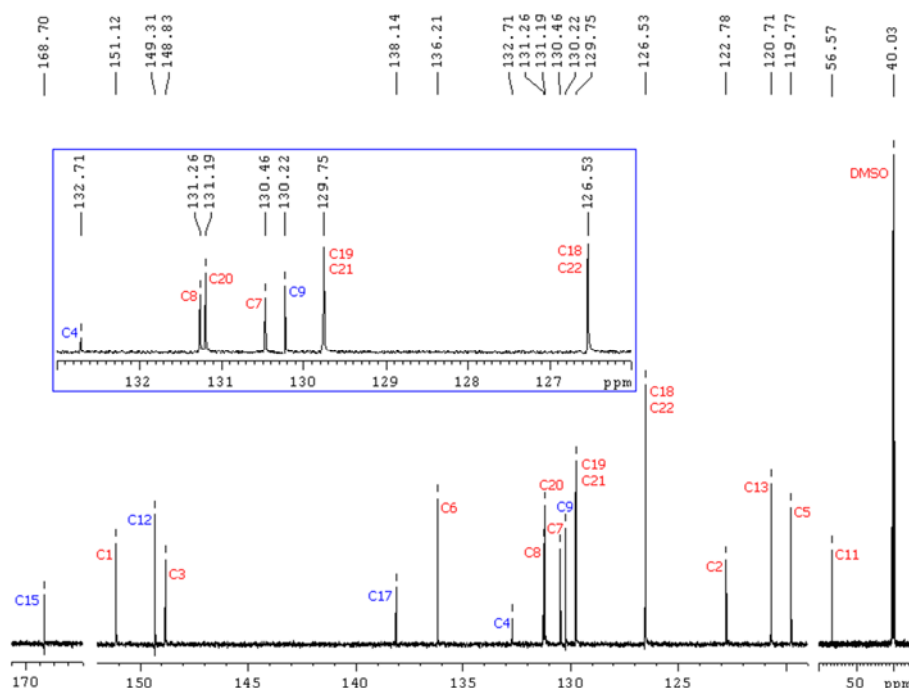


Fig. 6 –  $^{13}\text{C}$  NMR spectrum of 2PTMQI molecule; inset: details zoom.

To correlate the  $^1\text{H}$  NMR and  $^{13}\text{C}$  NMR spectra, we used the  $^1\text{H}$ - $^{13}\text{C}$  HSQC NMR technique. The Heteronuclear Single Quantum Coherence (HSQC) is used in NMR spectroscopy of organic molecules [18]. The spectrum contains a peak for each unique proton attached to a  $^{13}\text{C}$  nucleus. The basic scheme of this experiment involves the transfer of magnetization on the proton to the  $^{13}\text{C}$  nucleus.

Thus, the 2D NMR spectrum shows several correlations between: C11 with H30, H31 (Figure 8a); C5 with H26; C13 with H32; C2 with H24; C18 and C22 with H33 and H37; C19 and C21 with H34 and H36; C7 with H28; C20 with H35; C8 with H29; C6 with H27; C3 with H25; C1 with H23 (Figure 8b).



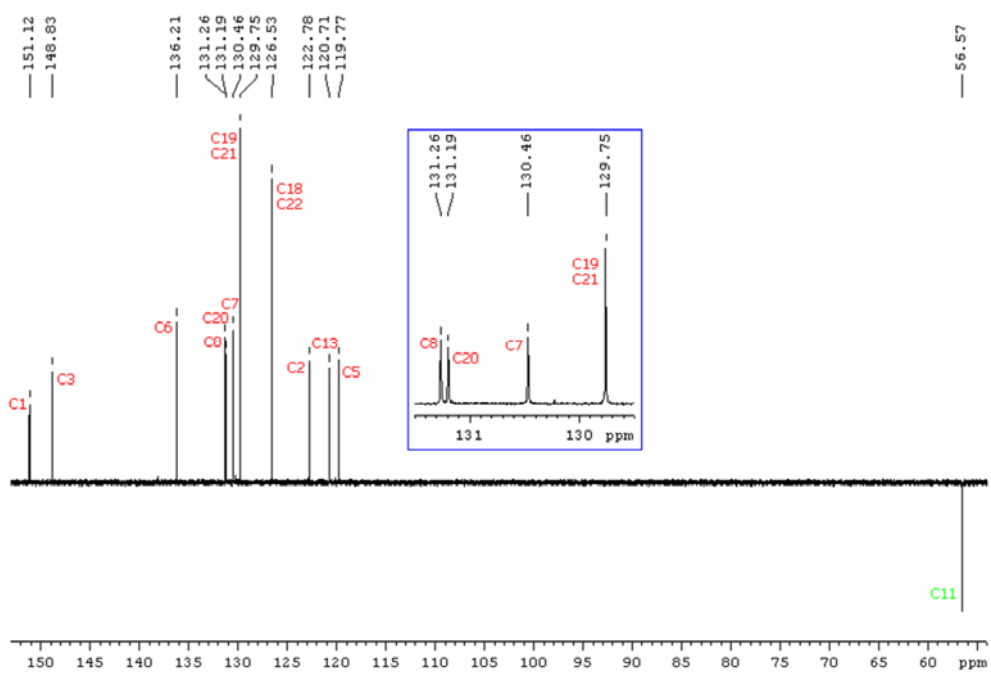
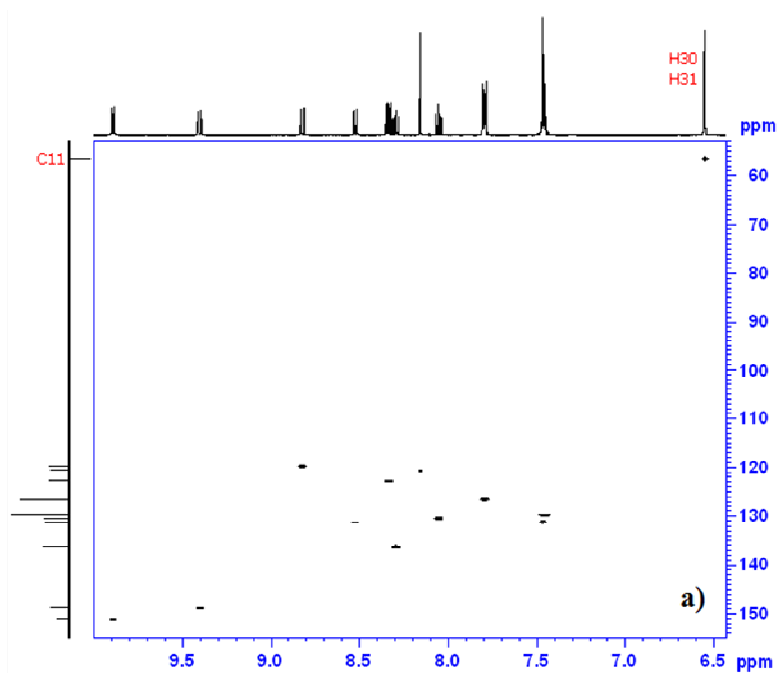


Fig. 7 –  $^{13}\text{C}$ -DEPT NMR spectrum of 2PTMQI molecule; inset: details zoom.



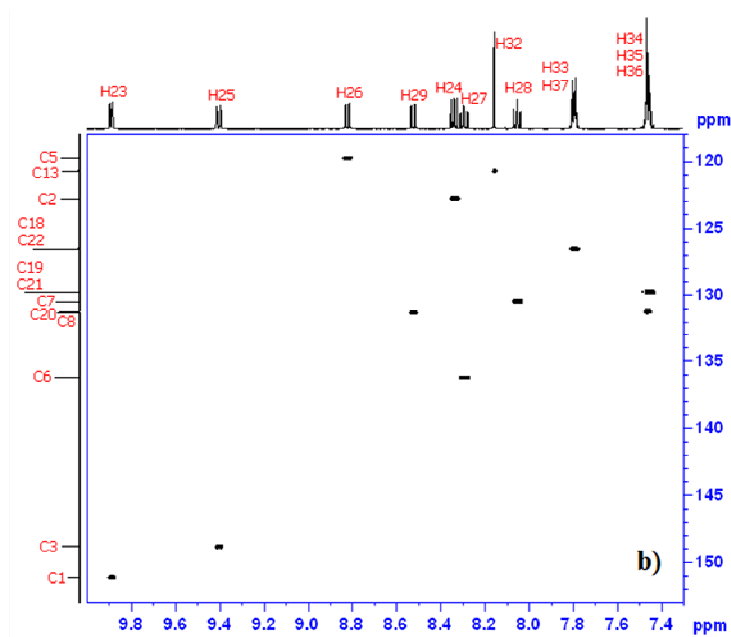


Fig. 8 –  $^1\text{H} - ^{13}\text{C}$  HSQC NMR spectrum of 2PTMQI molecule (a); details of 118–152 ppm for  $^{13}\text{C}$  (b).

#### 4. CONCLUSIONS

Crystal structure of the 2PTMQI molecule has been determined by X-ray diffraction technique. In liquid phase, the NMR spectra confirm the proposed structure and the NMR absorption signals were correctly assigned based on 2D correlation spectra ( $^1\text{H}-^1\text{H}$  COSY and  $^1\text{H}-^{13}\text{C}$  HSQC). The 2PTMQI molecule structure was obtained and interpreted correctly by using X-ray diffraction and NMR. It shows a very good correlation between the results obtained by the two methods.

*Acknowledgements.* This work was financially supported by UEFISCDI Romania, Project PCE-2011-3-0032.

#### REFERENCES

1. L. Szabo, V. Chis, A. Pîrnău, L. Leopold, O. Cozar, Sz. Orosz, J. Mol. Struct. **924-926**, 385–392 (2009).
2. C. Moldovan, O. Oniga, A. Pârveu, B. Tiperciuc, P. Verite, A. Pîrnău, O. Crisan, M. Bojita, R. Pop, Eur. J. Med. Chem. **46**, 526–534 (2011).
3. A. Pîrnău, V. Chiş, L. Szabo, O. Cozar, M. Vasilescu, O. Oniga, R. A. Varga, J. Mol. Struct. **924-926**, 361–370 (2009).

4. M. Komloova, K. Musilek, A. Horova, O. Holas, V. Dohnal, F. Gunn-Moore, K. Kuca, *Bioorg. Med. Chem. Lett.* **21**, 2505–2509 (2011).
5. K. Musilek, M. Komloova, V. Zavadova, O. Holas, M. Hrabnova, M. Pohanka, V. Dohnal, F. Nachon, M. Dolezal, K. Kuca, Y. S. Jung, *Bioorg. Med. Chem. Lett.* **20**, 1763–1766 (2010).
6. Q. S. Yu, H. W. Holloway, W. Luo, D. K. Lahiri, A. Brossi, N. H. Greig, *Bioorgan. Med. Chem.* **18**, 4687–4693 (2010).
7. K. Musilek, M. Komloova, V. Zavadova, O. Holas, M. Hrabnova, M. Pohanka, V. Dohnal, F. Nachon, M. Dolezal, K. Kuca, *Eur. J. Med. Chem.* **46**, 811–818 (2011).
8. S. K. Bharti, G. Nath, R. Tilak, S. K. Singh, *Eur. J. Med. Chem.* **4**, 651–660 (2010).
9. J. M. Beale, J. H. Block, *Wilson's and Gisvold's textbook of organic medicinal and pharmaceutical Chemistry* 12<sup>th</sup> ed, Lippincott Williams and Wilkins, Philadelphia, 2011.
10. M. Palage, S. Oniga, A. Pîrnău, V. Zaharia, C. Belegan, L. Vlase, A. Mureşan, *Farmacia* **57**, 598–608 (2009).
11. I. Ielciu, O. Voştinaru, S. Oniga, C. Mogoşan, L. Vlase, A. Pîrnău, C. Araniciu, M. Palage, *Dig. J. Nanomater. Bios.* **8**, 1089–1099 (2013).
12. G. M. Sheldrick, *Acta Cryst* **A64**, 112–122 (2008).
13. M. Billeter, *Persp. Drug Discov. Des.* **3**, 151–167 (1995).
14. L. J. Farrugia, *J. Appl. Cryst* **30**, 565–566 (1997).
15. K. Brandenburg, *DIAMOND. Release 3.0*, Crystal Impact GbR, Bonn, Germany, 2006.
16. D. Soto-Castro, A. Evangelista-Lara, P. Guadarrama, *Tetrahedron* **62**, 12116–12125 (2006).
17. H. E. Gottlieb, V. Kotlyar, A. Nudelman, *J. Org. Chem.* **62**, 7512–7515 (1997).
18. H. Friebolin, *Basic One and Two Dimensional NMR Spectroscopy*, Weinheim Wiley-VCH, 2005.